# COMPLEX PORE GEOMETRIES IN NATURAL BUILDING STONES: AN EXPERIMENTAL AND THEORETICAL APPROACH FOR THE MODELING OF POROSITY CHANGES IN NATURAL, DEGRADED AND TREATED CALCARENITES

SIMONA RANERI

Dipartimento di Scienze Biologiche, Geologiche e Ambientali, Università di Catania, Corso Italia 57, 95129 Catania

INTRODUCTION

The durability of natural building stones subjected to weathering processes is a current issue in geological, engineering, and conservation fields in the perspective of preserving Cultural Heritages. The esteem of this parameter is strongly related to several features of the rocks, namely mineralogical, petrographic, chemical, textural, and physical-mechanical proprieties, including pore structure. Among them, the description of the pore structure is one of the more difficult to obtain, because of the complex geometry of pore network of stones, as well as the variability of the size distribution of voids (ranging from nanometers to millimeters; Barbera *et al.*, 2014). Moreover, the quantification of the changes in the pore structure and surface texture due to degradation processes represents a key element in the correct interpretation of stone behavior (Turkington & Paradise, 2005) and in the proper application of conservative treatments in the framework of restoration works.

In recent years, the use of innovative, non-invasive and non-destructive techniques able to characterize both sub-surface and surface features of porous materials has largely increased, especially in stone conservation studies. Neutron and X-Ray imaging methods have been proved to be valuable procedures for the characterization of archaeological, geological, and industrial materials (Cnudde & Boone, 2013; Perfect *et al.*, 2014). In fact, the results of the imaging analyses are not limited to a simple 2D or 3D representation of the studied objects, as a large amount of quantitative information can be also obtained. Nuclear Magnetic Resonance (NMR) applications have been also widely used to study the petrophysical features of rock materials, especially porosity and permeability (Capitani *et al.*, 2012). Finally, non-destructive digital image techniques have provided as new tools for measuring changes in stone surfaces (Moses *et al.*, 2014), assuring a high resolution and the possibility to monitor the measured parameters over the time. This aspect is of a great interest in weathering studies, as surface represents the direct interface with atmosphere and, therefore, with the weathering agents.

Because of the aforementioned, this research was devoted to inspect the surface texture and sub-surface structure changes due to salt weathering in natural building stones employed in Cultural Heritages and to investigate the efficiency of innovative nano-structured products for stone protection and conservation. In detail, a theoretical and empirical approach based on non-invasive and non-destructive methods was applied, in order to: *i*) highlight the potential of classical and innovative complementary methods in quantifying the structural changes in porous materials due to degradation processes and conservative treatments; *ii*) validate the use of geometrical models in describing complex pore systems; *iii*) explain how innovative methods can help to facilitate the understanding of stone weathering; *iv*) expand the frontiers of the scientific knowledge in weathering studies; *v*) support the researches in the field of Cultural Heritages conservation and protection.

MATERIALS AND METHODS

Calcarenites are the most used building stones in Sicily, especially in the Southeast area of the island, in view of their suitable proprieties, as availability, color, easy extractability and good workability. They are also characterized by a wide range of pores and a complex porous structure. Various typologies of Oligocene-Miocene limestone and Pliocene sandstones have been used over the time in the local masonry (Anania *et al.*, 2012). Among them, of particular interest is a coarse grained and yellowish calcarenite, namely *Sabucina Stone* (Fig. 1a-c),

recently used to replace stone in several Sicilian Cultural Heritages because of its peculiar aesthetical and physical-mechanical proprieties (Bellanca *et al.*, 1999). In view of the aforementioned, it was selected for this study.
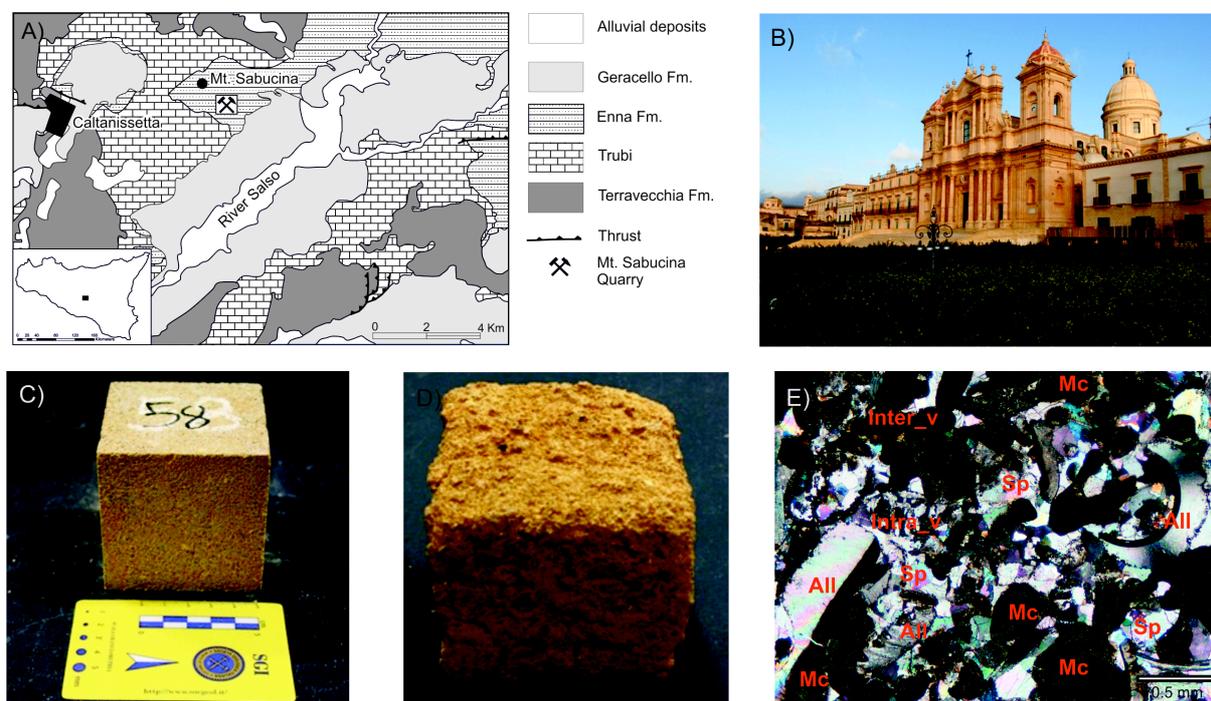


Fig. 1. - (a) Geological sketch map and localization of the quarried area of Sabucina Stone; (b) example of the use of Sabucina Stone in monuments of Sicily (Noto Cathedraly); (c) fresh sample of Sabucina Stone; (d) picture of Sabucina Stone sample at the end of the accelerated aging tests UNI EN 12370; (e) microphotographs of Sabucina Stone (Abbreviations: All, allochems; Sp, sparite; Mc, micrite; Inter_v, inter-particle voids; Intra_v: intra particle voids).

A preliminary characterization of Sabucina Stone from the petrographic, mineralogical, geochemical, physical, and mechanical point of view was performed by applying a classical methodological routine based on standard recommendations. Thus, several samples of Sabucina Stone were artificially weathered according to the UNI EN 12370 standard on the resistance of natural stones to crystallization damage (Fig. 1d). Fresh and degraded samples at different salt crystallization steps were therefore analyzed by using classical (*i.e.*, physical-mechanical tests and porosimetric analysis by mercury intrusion) and non-invasive and non-destructive methods (*i.e.*, X-Ray μ-CT, neutron imaging, portable NMR and 3D digital microscopy) in order to visualize, quantify and model the changes in sub-surface and surface features of the stone due to salt weathering processes. Noteworthy, tests and analyses were carried out on samples with different dimension in order to evaluate the possible dimensional effects of weathering on the stone.

Firstly, mercury intrusion porosimetry (MIP) measurements were performed on artificially weathered and cleaned samples subjected to different weathering cycles in order to highlight the difference in pore network arrangement due to salts crystallization over different degradation degree. In detail, Thermo Scientific™ Pascal 140 and 240 Mercury Porosimeters (maximum pressure of 400 kPa and 200 MPa, respectively) were used and measurements were performed on small samples similar in dimension and shape. Data were processed by using ThermoFisher software SOL.I.D (Solver of Intrusion Data) and analysed in view of appropriate empirical models.

The quantification and visualization of pore changes were also obtained by using non-destructive methods. In particular, X-ray tomographic scans were acquired at the Centre for X-ray Tomography (UGCT; Ghent University, Belgium) by using the HECTOR scanner. The obtained raw CT data were reconstructed with the UGCT Octopus software. For the 3D visualizations and the 3D quantification of pore network features (such

as equivalent diameter –ED- and maximum opening – OM) VGStudio MAX (Volume Graphics) and the UGCT software tool Morpho+ were used, respectively. Additionally, nuclear magnetic resonance measurements (NMR) were performed at the Laboratory of Nuclear Magnetic Resonance Anna Laura Segre of the Chemical Methodologies Institute of CNR in Rome; for the experiments, a portable single-sided NMR sensor by RWTH Aachen University (Germany) was used. Transversal relaxation times $T_2$ were measured and the variations in spin population of the $T_2$ components were evaluated.

The effects of salts weathering on physical proprieties and mechanical resistance of the rocks were investigated by performing standard tests (*i.e.*, mechanical resistance, ultrasound velocity, density) on samples subjected to different artificial degradation steps; then, the influence of microtextural and microstructural modifications related to salt crystallization in the engineering properties of the studied rock was evaluated.

Moreover, the influence of the pore structure changes in fluid flow through porous network of the stone was studied by using neutron imaging at the IMAGINE beamline situated at the Laboratoire Léon Brillouin (CEA/CNRS) in Saclay (France). In particular, neutron radiographies were acquired in dynamic set-ups by monitoring the capillary absorption process in Sabucina Stone as function of time and weathering degree. Parameters as effective capillary radius and sorptivity were calculated by using the intrusion depth of the waterfront in function of time. In order to quantify the water content distribution (in percentage) inside the stone, radiographs were processes according to Kim *et al.* (2012). Neutron tomographies were also acquired in order to obtain a multi-dimensional investigation of water uptake process.

Changes in surface roughness parameters were esteemed on sample subjected to different degradation degree by performing surface morphometrical analyses on unweathered and weathered samples of Sabucina Stone. 3D images of the surfaces were acquired by using Hirox KH-7700 digital microscope with an MXG-10C body, an OL-140II lens and an AD-10S Directional Lighting Adapter at the University of Siena (Italy). The acquired images were processes by using the ImageJ plug-in SurfCharJ and surface texture parameters and profiles (both in term of roughness and waviness) were obtained.

Finally, the fractal dimension of pore surface was calculated on the basis of porosimetric data.

The overall of the obtained results were compared and interpreted according to appropriate empirical models and employed for planning conservative treatments devoted to coarse-grained calcarenite substrates.

In this framework, innovative protective and consolidant products based on sol-gel process were synthesized at Department of Chemistry in University of Parma (Bergamonti *et al.*, 2014) and tested on Sabucina Stone. The products consisted in: *i*) self-cleaning photocatalytic nanoparticles $TiO_2$-based surface coatings and *ii*) hybrid organic-inorganic products (*i.e.*, a colloidal silica and silicone hydrophobic protective with fluorurate groups named WS3, a hybrid patented product[1] consisting in minopropyltriethoxisilane with a functional silicon-alkoxide group named PAASi and a hybrid sol based on an Al-Si network functionalized with organic chains named AlSiX). In order to verify the compatibility of the products with calcarenite substrates, efficiency tests were performed by using a routine based on standard recommendations. Moreover, in order to visualize the penetration depth and the distribution of the investigated products inside the studied stone, comparative mercury intrusion porosimety analyses, X-ray tomography and neutron imaging measurements were performed on treated stone samples. Finally, referring to protective products based on $TiO_2$ nanoparticles, surface modifications were evaluated by performing digital surface morphometric measurements.

RESULTS AND DISCUSSIONS

*Characterization of Sabucina Stone*

From the petrographic point of view, Sabucina stone exhibited a microscopic texture varying between grainstone and packstone, due to the irregular distribution of sparite and micrite, the latter being enriched in iron oxides and thus responsible for the stone color. Allochems are mainly formed by small fragments (200 μm - 2,5 mm in

---

[1] Bergamonti L., Chappini E., Maistrello L., Palanti S., Predieri G., Wood preservative compositions, WO 2015004590 A1

dimension) of Mollusca and orthochems were due to irregularly distributed sparitic calcite and micrite; a silicoclastic component (2-3%), composed by sub-rounded grains of quartz (100 μm in diameter on average) is also present. The porosity, mainly interparticle moldig and vuggy, is of about 27%. Petrographically, the stone is a biosparite (Fig. 1e). It is mainly isotropic and no orientation of the bedding is visible at outcrops or by macroscopic and microscopic inspection. The mineral matrix is composed primarily of calcium carbonate (~ 90%), with quartz (~ 5%) and dolomite (~ 4%).

Porosimetric data, physical and mechanical proprieties obtained on Sabucina Stone on the basis of standard recommendations are summarized in Table 1.

Table 1 - Porosimetric data, physical and mechanical proprieties of Sabucina Stone.

| Porosimetric data[1] | | | | Physical proprieties | | | | | |
|---|---|---|---|---|---|---|---|---|---|
| Total accessible porosity (%) | Total pore volume (g/cm³) | Average pore radius (μm) | Mode peak (μm) | Capillarity coefficient[2] (g/cm²) | Immersion absorption coefficient[3] (%) | Dry index coefficient[4] (%) | Total weight loss[5] (%) | Saturation coefficient[6] (%) | Interconnection among pores[7] (%) |
| 26.86 | 0.1356 | 0.1442 | 8.5567 | 0.02 | 11.07 | 0.4 | -11.09 | 71.80 | 22 |
| Mechanical proprieties | | | Vp (dry) | | Vp (wet) | | Physical parameters | | |
| UCS dry[8] (MPa) | UCS wet[9] (MPa) | Flexural strength[10] (MPa) | Mean velocity[11] (m/s) | Anisotropy[12] (%) | Mean velocity (m/s) | Anisotropy (%) | Real and apparent density[13] (g/cm³) | Total and effective porosity[11] (%) | Imbibition coefficient[11] (%) |
| 6.12±0.8 | 5.80±1.25 | 6.53±1.4 | 2040 ±46.16 | 7.09% | 3042 ±77.2 | 9.09 | 2.67 - 1.87 | 30-29 | 13 - 16 |

[1]MIP measurements; [2]NORMAL 11/88; [3]NORMAL 7/81; [4]NORMAL 29/88; [5]UNI EN 12370 (2001); [6]Cultrone *et al.* (2003); [7]RILEM (1980); [8]UNI EN 1926 (2000); [9]UNI EN 1926 (2000); [10]UNI EN 12372 (2001); [11]NORMAL 22/86; [12]Birch F. (1961); [13]UNI EN 1936 (2001).

*Quantification and visualization of pore structure, surface texture and physical-mechanical features variations due to salt weathering*

Comparative measurements on fresh and artificially degraded samples at different artificially degradation steps were performed in order to evaluate the surface texture and sub-surface structure variations due to salt weathering in the studied stone (Fig. 2 and Table 2).
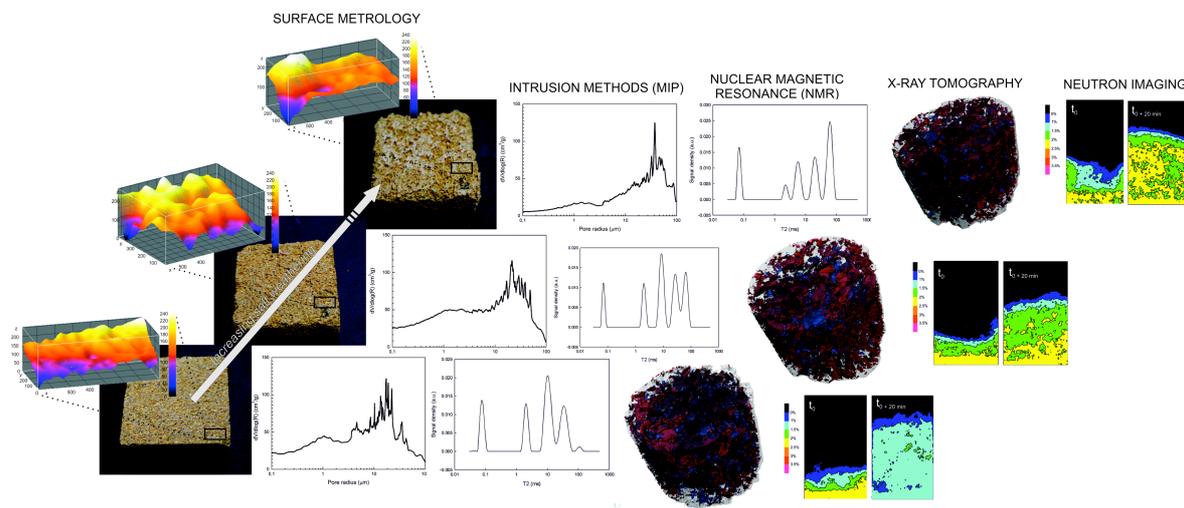


Fig. 2 - Schematic overview of the results obtained on different samples of Sabucina Stone by applying an integrate methodological approach. The results about fresh and artificially degraded samples subjected to eight and fifteen salts crystallization cycles are reported, as examples.

First of all, the application of classical intrusion method as MIP and the subsequent treatment of data according to Angeli *et al.* (2007) allowed to obtain information on weathering mechanism as well as on location

of salts. The results allowed us to obtain a good explanation of the degradation style of the stone, giving back an interesting correlation between the mass loss curves and the weathering mechanism suggested by porosimetric data. In fact, from the 1st to the 6th cycles the curve was "salt controlled" (positive mass variation) and the porosimetric curves suggested the crystallization of salts in the entry of pores, whereas from the 7th cycle the curve was "weathered controlled" (negative mass variation), with an increasing of the throats radius and the crystallization of salts inside the enlarged pores. In fact, the modal pore radius shifted from a value of about 8 µm in the unweathered sample to 12 µm in the weathered ones, with a peak of 14 µm corresponding to a change in the degradation mechanism; in this framework, salts were located in pores ranging from 50 to 100 µm. Such a behavior affected also the physical-mechanical properties of the stone, whose parameters were subjected to significant variation with the advancement of the degradation process. In fact, a globally decrease of density and ultrasound velocity was observed, especially from the 6th salts crystallization cycle, even if a non homogeneous trend might be delineated. Referring to compressive strength, the measured UCS values exhibited a trend inversion in correspondence with the degradation mechanism change up to the 4th crystallization cycle; this trend might be explained with the supporting case of porosimetric measurements. In fact, from the 2nd to the 4th crystallization cycles, salts filled the pore throats, determining a slight and progressive increment of compressive strength resistance. Otherwise, when the enlargement of the throats and the filling of the pores occurred (*i.e.* up to 6th crystallization cycle) a decrease of UCS values was observed, claiming a strict relationship between the location of salts and the mechanical resistance of the stone (see also Barone *et al.*, 2015).

Table 2 - Main changes in porosimetric, physical and mechanical proprieties of Sabucina stone as a function of artificially salts weathering steps

| UNI EN 12370 | MIP | Portable-NMR | RILEM 1980 | | UNI EN 1936 | | | NORMAL 22/86 | UNI EN 1926 | X-ray µ-CT | | | Neutron radiography | Surface analysis | | Fractal dimension |
|---|---|---|---|---|---|---|---|---|---|---|---|---|---|---|---|---|
| N. salts crystallization cycles | Modal pore radius (µm) | Most significant $T_2$ and W | $A_s$ (%) | S (%) | Apparent density (g/cm³) | Real density (g/cm³) | Porosity (%) | Ultrasonic velocity (m/s) | UCS (MPa) | Open porosity (%) | Closed porosity (%) | Total porosity (%) | Sorpivity (mm/s⁰·⁵) | Roughness (Rq) | Waviness (Wq) | Pore surface |
| fresh | 8.557 (±3.088) | $T_{2C}$ 10.33 ms $W_C$ 40% | 22.44 | 71.80 | 2.04 | 2.77 | 26.24 | 2028.01±12.71 | 6.12 ±0.80 | 9.78884 | 1.5073 | 11.29614 | 0.300 | 7.3258 | 5.163 | 2.77 |
| 2 | 7.799 (±1.168) | | | | 2.02 | 2.76 | 26.70 | 1443.50±8.23 | 6.53±1.34 | | | | | | | |
| 4 | 14.693 (±2.81) | | 21.92 | 72.75 | 1.94 | 2.63 | 26.47 | 1463.00±4.62 | 7.72±1.16 | 8.64147 | 1.57003 | 10.2115 | 0.301 | 5.7352 | 5.9865 | 2.82 |
| 6 | 12.843 (±3.043) | | | | 2.01 | 2.61 | 22.81 | 1423.67±8.16 | 6.17±0.27 | | | | | | | 2.81 |
| 8 | 11.636 (±2.159) | $T_{2C}$ 8.74 ms $W_C$ 30% | 21.66 | 73.62 | 1.90 | 2.45 | 22.32 | 1200.00±6.14 | 7.41±4 | 7.42108 | 1.66482 | 9.0859 | 0.308 | 5.6189 | 4.3765 | 2.81 |
| 10 | 10.395 (±1.614) | | | | | | | | | | | | | | | 2.84 |
| 12 | 13.835 (±2.858) | | 22.14 | 73.21 | | | | | | 15.0476 | 0.94694 | 15.99454 | 0.373 | 8.2656 | 12.4268 | 2.9 |
| 15 | 12.694 (±3.516) | $T_{2E}$ 62.95 ms $W_E$ 40% | 21.39 | 77.47 | | | | | | 14.4407 | 0.7458 | 15.1865 | 0.366 | 4.7365 | 10.9475 | 2.9 |

Beside the successfully results obtained by applying the aforementioned destructive and micro-destructive methods, the use of innovative methods allowed to obtain additionally and more accurate data. In this sense, the application of portable single side NMR confirmed the trends obtained by MIP measurements. In fact, the analyses of transverse relaxation times ($T_2$) and their distributions highlighted that: *i*) the decay constant $T_2$ was proportional to the pore size with small pores characterized by relaxation times shorter than those measured in large pores; *ii*) Sabucina fresh sample showed a whole of five component of $T_2$ with the more populated centered in the medium pores size (about the 50% of population density was centered at ~ 10 ms); *iii*) as the number of weathering cycles increased, the longest component of $T_2$ (at about 60 ms) reached the 40% of the total pore size population, indicating an increase of the largest pores (Di Tullio *et al.*, 2015).

However, all the aforementioned methods did not allow the visual inspection of both processes and the effects related to the weathering action; therefore, imaging methods were employed. In detail, by using X-ray µ-CT the pore network modification due to weathering was visualized and quantified through parameters as total, open and closed porosity, equivalent diameter (ED) and maximum opening (MO). The obtained results suggested that, in general, salt crystallization determined the increase of the total porosity (*i.e.*, from 11.30% in a

fresh sample to 15.19% after 15 weathering cycles), with the creation of cracks and enlargement of pores. The open porosity increased from 9.78% to 14.44% over the crystallization cycles, whereas the closed porosity decreased with the induced degradation (*i.e.*, from 1.50% in a fresh sample to 0.75% after 15 crystallization cycles). Overall, the enlarged pores in weathered samples exhibited higher MO and ED values than the freshly quarried sample. The main dimensional changes covered the range of pores with ED > 1000 μm, with an increase up to 50% of the total porosity and, consequently, a decrease in porosity with ED between 100 and 1000 μm; moreover, the porosity attributed to pores with ED < 100 μm drastically decreased. In regard to MO, the percentage of pores with an MO value < 150 μm decreased to 49%, 38% and 30-20% from 4 to 15 cycles, respectively, whereas an increase of the range between 150 and 350 μm was observed (from ~ 50% to 63% from 4 to 15 cycles). Noteworthy, the range > 350 μm was present only in the samples submitted to 12 and 15 crystallization cycles, contributing to ~ 30% of the total porosity (see also Raneri *et al.*, 2015).

As far as the pores were enlarged, the stone became able to absorb much more water, as testified by the increasing of the saturation coefficient (*i.e.*, from 71.80% to 77.47%) calculated in samples subjected to different degradation steps. However, the comparison between interconnection parameter in unweathered and weathered samples highlighted that the salt weathering process did not alter the ability of the stone to vehicle moisture (mean value of about 22%). These evidences are enforced by the results obtained by neutron imaging tests (see also Raneri *et al.*, 2016).

The analysis of raw neutron images highlighted a link between the speed of the wetting front and degradation degree of the samples. In fact, the more degraded the sample was, the faster the wetting front advanced; moreover, non-planar waterfronts in degraded samples might be observed, suggesting the modification of the morphology of the pore network (pore size distribution and connectivity) due to weathering processes with consequent different capillary properties. In order to better understand the dynamics of water observed in the raw radiographs, reference dry and wet images were evaluated for the mass thickness of water.

Contours, describing the quantitative distribution of water inside the stone volumes, clearly showed the presence of different flow paths over the time. In detail, changes in pore network due to weathering were responsible for a modification of the water distribution; it appeared non-homogeneous with the assessment of areas of higher WC% percentage than the surrounding. Additionally, in weathered samples, the faster advancement of the wetting front was associated with a higher amount of absorbed water, evidencing a modification in the accessible porosity.

Finally, side effects due to more intense action of the degradation process close to the surface, was evidenced by the fast advancement of the wetting front and the high WC% at the edges of the weathered stone samples compared with the inner part. All the aforementioned are better visualized in neutron tomographies for the occurrence of differential flow patterns inside the whole of investigated volume of weathered samples.

The more intense action of weathering on surface was also claimed by a significant change of roughness and waviness parameters measured by 3D digital microscopy. In detail, by monitoring the roughness changes over the different artificially weathering cycles, a decrease of roughness parameters and profiles was observed, claiming a smoothing of the surface evaluated at smaller wavelengths. On the contrary, an increasing of longer-length ondulation structures was observed (waviness parameters and profiles). Therefore, as the weathering process proceeded, the granular disintegration and powdering of the surface determines a decrease of shorter-length ondulation and, at the same time, an increase of the longer wavelength component.

*Use of fractal models to describe pore structure of building stones*

Starting from porosimetric analyses performed on fresh, weathered and cleaned samples of Sabucina Stone, the fractal dimension of pore surface was extracted following the surface fractal model by Friesen & Mikula (1987). According to it, the cumulative intrusion volume derivative with respect to pressure and the surface fractal dimension D are related by the relation:

$$\log(dV/dP) \propto (D-4)\log(P)$$

being V the cumulative intrusion volume at a given pressure P. By using this relation, the surface fractal dimension might be easily calculated; in fact, plotting the logarithm of derivative cumulative intrusion volume *vs*. pressure logarithm, if pore surface is fractal in a specific range of pore diameters, a linear tendency can be observed and *D* is obtained from the slope of that line.

The obtained parameters (Table 2) indicate that the weathering process determine a progressive increase of pore surface fractal dimension, *i.e.* from 2.77 in fresh samples to 2.90 in weathered samples and to 2.92 for cleaned ones (at the end of the 14 cycles). Considering that the fractal dimension describe the complexity of the pore surface, the obtained behavior suggests a progressive increasing of pore complexity, maybe due to the presence of salts, in weathered samples, and the appearance of new pores, in cleaned samples.

*Innovative protective and consolidant products: efficiency tests*

Water based sols containing titanium dioxide were deposited on Sabucina stone to obtain self-cleaning coatings, taking advantage of the well known $TiO_2$ photocatalytic properties. Basic (TiMaA) and acid (TiAcN) sols were synthesized by sol-gel method, working at low temperatures and in different environments, with the aim to evaluate the effects of sols at different pH on calcarenite substrate (Bergamonti *et al.*, 2015). The $TiO_2$ obtained were principally made of anatase with a few percent of brookite. As the use of coatings with a self-cleaning activity on architectural elements requires that they do not alter the original aspect of stone substrates and do not produce physical and chemical changes, morphological observations and several efficiency tests (*e.g.,* colorimetric-, photocatalytic-, comparative water absorption-, and accelerated aging-tests,) were carried out according to UNI-EN standards. The obtained results highlighted that both acid and basic titanium nanosols exhibited good properties, in terms of preserving the characteristics of the stone; in fact, the treatments did not significantly alter the color ($\Delta E$ about of 1.5) and the water absorption proprieties of the studied material. Referring to the durability of the stone, the resistance to salt crystallization was generally improved, as showed by accelerated degradation test. As concern the self-cleaning properties, both $TiO_2$ coatings exhibited a good photodegradation activity on methylene blue and methyl orange dyes; however, a better efficiency of the basic preparation (TiMaA) under UV lamp and the acid preparation (TiAcN) under daylight one has to be claimed.

Hybrid products (consolidant PAASi and AlSiX, associated with the hydrophobic coating WS3) were also tested on Sabucina Stone and efficiency tests were carried out according to standard recommendations (Fig. 3.a; Alfieri *et al.*, 2014).

The obtained results highlighted that the silicon alkoxide product (AlSiX) determined strong chromatic changes, especially when used in association with the hydrophobic coating, as well as a slightly decrease of resistance of stone against salts crystallization. Otherwise, the use of polyammidoammine-based product (PAASi) seemed to be less invasive in term of chromatic changes, assuring at the same time a lower absorption of water by capillarity and total immersion as well as a significant enhancement of durability of the stone against salt crystallization weathering. Finally, the overall of the obtained data on treated samples coated also with the hydrophobic product (WS3) claimed an improvement of the performances of both consolidants respect to the usage by themselves, even if a slight decrease of the salt crystallization resistance has to be claimed.

*Quantification of pore structure and surface texture modifications due to protective and consolidant treatments*

The investigation of additional aspects as penetration depth and interaction with substrate of the tested products were achieved by a multi-scalar and multi-methodological approach. In detail, several methods (MIP, X-ray μ-CT, neutron radiography, 3D surface microscopy) were applied (Fig. 3b-c) in order to: *i*) evaluate the penetration depth of AlSiX and PAASi consolidant (used also in combination with WS3 hydrophobic treatment), *ii*) quantify and visualize the possible modification of the behavior of the stone against water, and *iii*) esteem the surface texture changes in samples coated with $TiO_2$ nano-sols.

Referring to the consolidant treatments, the results derived from the application of intrusion mercury method were not convincing, maybe due to the limits of resolution in term of investigable pore size. Otherwise, better results were obtained by using X-ray μ-CT. In fact, the technique allowed to quantify the impregnation of

PAASi in a range of 10 µm < ED < 100µm and MO < 50 µm and the distribution of AlSiX product in a larger pore range (ED between 100 and 500 µm; MO between 50 and 150 µm), claiming a different interaction of the products with the pore network structure of the stone.
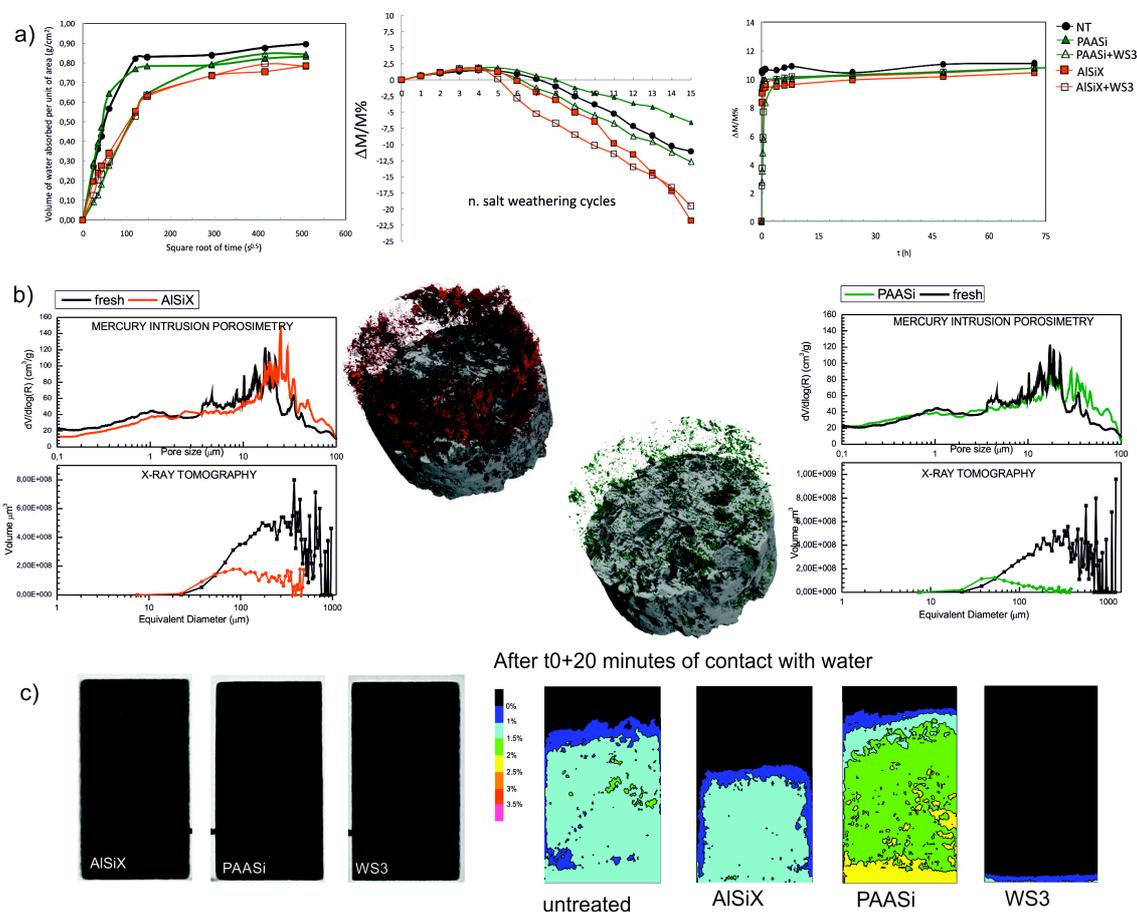


Fig. 3 - Schematic overview of the results obtained on treated samples of Sabucina Stone. (a) Results of efficiency test based on standard recommendation routine; (b) porosimetric data obtained by classical intrusion methods (MIP) and X-ray micro-tomography along with 3D volume rendering of the treated and scanned cores; (c) raw neutron radiographs and water content percentage contouring of treated samples.

More complete description was obtained by using neutron radiography, due to its high sensitivity to hydrogen-based materials. In particular, for AlSiX a penetration depth of about 2-3 mm was esteemed, whereas PAASi and hydrophobic products were impossible to visualize. In spite of the scarce penetration depth, the products affected the hydric proprieties of stone. In fact, the monitoring of capillary uptake over the time and the determination of the relative sorptivity coefficients highlighted that in samples treated with AlSiX the penetration of water was slightly inhibited by the presence of the product; otherwise, the PAASi treatment determined any significant change with respect to the untreated stone. Finally, in the case of hydrophobic product, the radiographs images convincingly illustrated that no water invaded the stone samples, also when it was used in association with the consolidants. The previous qualitative information were confirmed by the quantification of water percentage distribution inside the treated samples. In fact, the WC% contour plots showed a significant reduction of water absorption by capillarity in the stone samples treated with AlSiX consolidant (always, the WC values were < 2%), whereas in the case of PAASi a slight worsening of the water resistance to absorption by capillarity was observed (values up higher than in the untreated stones, up to 2.5-3 WC%, were obtained). In the case of hydrophobic treatment, used both alone and in combination with

consolidants, the contour plots showed that water did not invade the samples over the monitoring time. Good agreement between data obtained from neutron radiography images and classical gravimetric tests was observed, having the former method the great advantage to visualize the process occurring inside the samples.

Finally, the morphometrical analyses performed on $TiO_2$-sols coated surfaces evidenced an overall decrease of surface roughness and waviness parameters, with a greater variation for the $TiO_2$ acid preparation, presumably more invasive on calcarenite substrates.

CONCLUSIONS

In this research, an experimental and theoretical approach based on the application of both classical and innovative and non-invasive techniques was tested in order to supply a complete model on porosity changes due to degradation process and conservative treatment in natural building stones. This approach was applied on a coarse-grained calcarenite, namely Sabucina Stone (Caltanissetta, Sicily, Italy), widely used as building material in Sicily and particularly suitable for this study as its complex pore geometry.

The overall of the obtained results suggested that the studied system (both in term of sub-surface and surface features) become more complex with the advancement of salt weathering process; in fact, surface was smoothed in term of small scale ondulation structures, new ranges of pores appeared, part of closed porosity was opened and therefore became accessible to moisture flow, water spread rapidly in the pore network thanks also to the presence of enlarged pores and, finally, the new structural arrangement caused the development of preferential water uptake fluid-flow patterns. Such a behavior was successfully described by using fractal models, as testified by changes in fractal dimension of the calculated pore surface values.

As aspects such process operating, weathering mechanism, stone response and quantification of damage were clarified, interesting implication about the complicate relationships between rate and scale were also concluded. On the whole, all methods suggested that in the studied stone the most intense effects of the degradation occurred up to the $4^{th}$ - $6^{th}$ crystallization cycles (giving therefore information on rate) and that the salts crystallization process was independent from the scale, as comparable results were obtained on samples exhibiting different dimension and shape used in the different experimental setups.

Finally, referring to the tested protectives and consolidants, the obtained results highlighted a good compatibility of the products on calcarenite substrate, even if some performances still need to be improved.

In conclusion, this research can be considered a good example of the potential of the applied experimental and theoretical approach in investigating how salt weathering process acts and in visualizing and quantifying pore structure and surface texture modifications due to protective and consolidant treatments in natural building stones, especially in the case of coarse-grained calcite-based materials. In addition, the study highlighted how by applying interdisciplinary, multi-scale and multi-methodological approach in complex systems more relationships can be understood, more questions answered and new questions asked. Therefore, answers to questions associated with how building stones change and how decaying masonry may be conserved can practically help the conservation science disciplines in continuing, evolving and maturing the researches in the stone weathering field.

REFERENCES

Alfieri, I., Barone, G., Bergamonti, L., Lorenzi, A., Lottici, P.P., Mazzoleni, P., Predieri, G., Raneri, S. (2014): Self-cleaning photocatalytic coating and hybrid organic-inorganic strengthen products for the protection and conservation of calcarenites from Sabucina (Italy, Sicily). *IMA 2014*, Johannesburg (South Africa).

Anania, L., Badalà, A., Barone, G., Belfiore, C., Calabrò, C., Mazzoleni, P., Pezzino, A. (2012): The stones in monumental masonry buildings of the "Val di Noto" area: New data on the relationships between petrographic characters and physical-mechanical properties. *Constr. Build. Mater.*, **33**, 122-132.

Angeli, M., Bigas, J.P., Benavente, D., Menéndez, B., Hébert, R., David, C. (2007): Salt crystallization in pores: quantification and estimation of damage. *Environ. Geol.*, **52**, 213-205.

Barbera, G., Barone, G., Crupi, V., Longo, F., Majolino, D., Mazzoleni, P., Raneri, S., Teixeira, J., Venuti, V. (2014): A multi-technique approach for the determination of the porous structure of building stone. *Eur. J. Mineral.*, **26**, 189-198.

Barone, G., Mazzoleni, P., Pappalardo, G., Raneri, S. (2015): Microtextural and microstructural influence on the changes of physical and mechanical proprieties related to salts crystallization weathering in natural building stones. The example of Sabucina stone (Sicily). *Constr. Build. Mater.*, **95**, 355-365.

Bellanca, A., Curcuruto, E., Lo Bue, S., Neri, R. (1999): Petrografia, geochimica e riferimenti all'impiego storico delle calcareniti plioceniche di Sabucina, Sicilia Centrale. *Miner. Petr. Acta*, **42**, 210-193.

Bergamonti, L., Alfieri, I., Franzò, M., Lorenzi, L., Montenero, A., Predieri, G., Raganato, M., Calia, A., Lazzarini, L., Bersani, D., Lottici, P.P. (2014): Synthesis and characterization of nanocrystalline $TiO_2$ with application as photoactive coating on stones. *Environ. Sci. Pollut. R.*, **21**, 13264-13277.

Bergamonti, L., Alfieri, I., Lorenzi, A., Predieri, G., Barone, G., Gemelli, G., Mazzoleni, P., Raneri, S., Bersani, D., Lottici, P.P. (2015): Nanocrystalline $TiO_2$ coatings by sol-gel: photocatalytic activity on Pietra di Noto biocalcarenite. *J. Sol-Gel Sci. Techn.*, **75**, 141-151.

Birch, F. (1961): The velocity of compressional waves in rocks to 10 Kbar: Part 2. *J. Geophys. Res.*, **66**, 2199-2224.

Capitani, D., Di Tullio, V., Proietti, N. (2012): Nuclear magnetic resonance to characterize and monitor cultural heritage. *Prog. Nucl. Mag. Res. Sp.*, **64**, 29-69.

Cnudde, V. & Boone, M. (2013): High-resolution X-ray computed tomography in geosciences: a review of the current technology and applications. *Earth-Sci. Rev.*, **123**, 1-17.

Cultrone, G., de la Torre, M.J., Sebastián, E., Cazalla, O. (2003): Evaluación de la durabilidad de ladrillos mediante técnicas destructivas (TD) y no-destructivas (TND). *Mater. Construcc.*, **53**, 41-59.

Di Tullio, V., Barone, G., Capitani, D., Proietti, N., Mazzoleni, P., Raneri, S., Giuffrida, A. (2015): Multiscale porosimetric description of pore network in building stones. *TECHNART 2015*, Catania (Italy).

Friesen, W.I. & Mikula, R.J. (1987): Fractal Dimensions of Coal Particles. *J. Colloid Interf. Sci.*, **120**, 263-271.

Kim, F.H., Penumadu, D., Hussey, D.S. (2012): Water distribution variation in partially saturated granular materials using neutron imaging. *J. Geotech. Geoenviron.*, **138**,147-154.

Moses, C., Robinson, D., Barlow, J. (2014): Methods for measuring rock surface weathering and erosion: A critical review. *Earth-Sci. Rev.*, **135**, 141-161.

Perfect, E., Cheng, C.L., Kanga, M., Bilheux, M.Z., Lamanna, J.M., Gragg, M.J., Wright, D.M. (2014): Neutron imaging of hydrogen-rich fluids in geomaterials and engineered porous media: A review. *Earth-Sci. Rev.*, **129**, 120-135.

Raneri, S., Cnudde, V., De Kock, T., Derluyn, H., Barone, G., Mazzoleni, P. (2015): X-ray computed micro-tomography to study the porous structure and degradation processes of a building stone from Sabucina (Sicily). *Eur. J. Mineral.*, **27**, 279-288.

Raneri, S., Barone, G., Mazzoleni, P., Rabot, E. (2016): Visualization and quantification of weathering effects and water uptake processes in natural building stones by using neutron imaging. *Appl. Phys. A*, DOI: 10.1007/s00339-016-0495-8.

RILEM (1980): Recommended test to measure the deterioration of stone and to assess the differences of treatment methods. *Mater. Struct.*, **13**, 175-253

Turkington, A.V. & Paradise, T.R. (2005): Sandstone weathering: a century of research and innovation. *Geomorphology*, **67**, 229-253.